ISCI, Volume *15*

Supplemental Information

EGFR Controls Hair Shaft Differentiation in a p53-Independent Manner

Nicole Amberg, Panagiota A. Sotiropoulou, Gerwin Heller, Beate M. Lichtenberger, Martin Holcmann, Bahar Camurdanoglu, Temenuschka Baykuscheva-Gentscheva, Cedric Blanpain, and Maria Sibilia

Fig. S1, Amberg et al

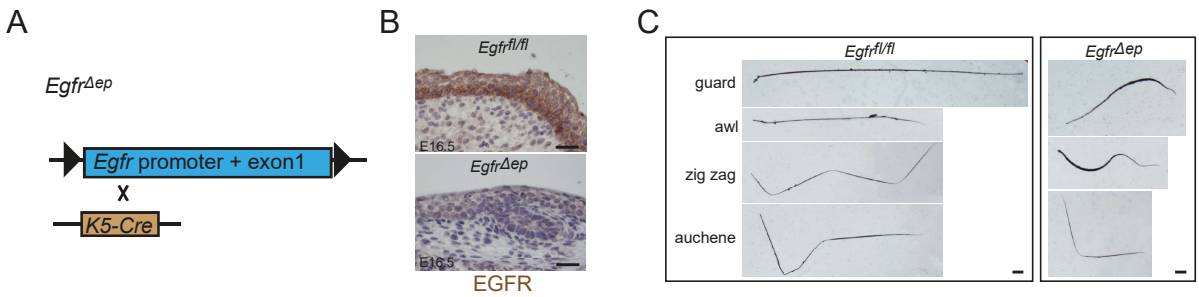

Figure S1. Loss of EGFR results in hair alterations. Related to Figure 1

(A) Schematic picture of *Egfr*$^{\Delta ep}$ mice.

(B) Immunohistochemistry staining of EGFR on sections of an E16.5 control and *Egfr*$^{\Delta ep}$ mouse.

(C) Brightfield images of plucked hair from P22 control and *Egfr*$^{\Delta ep}$ mice.

Scale bars 20μm unless otherwise stated.

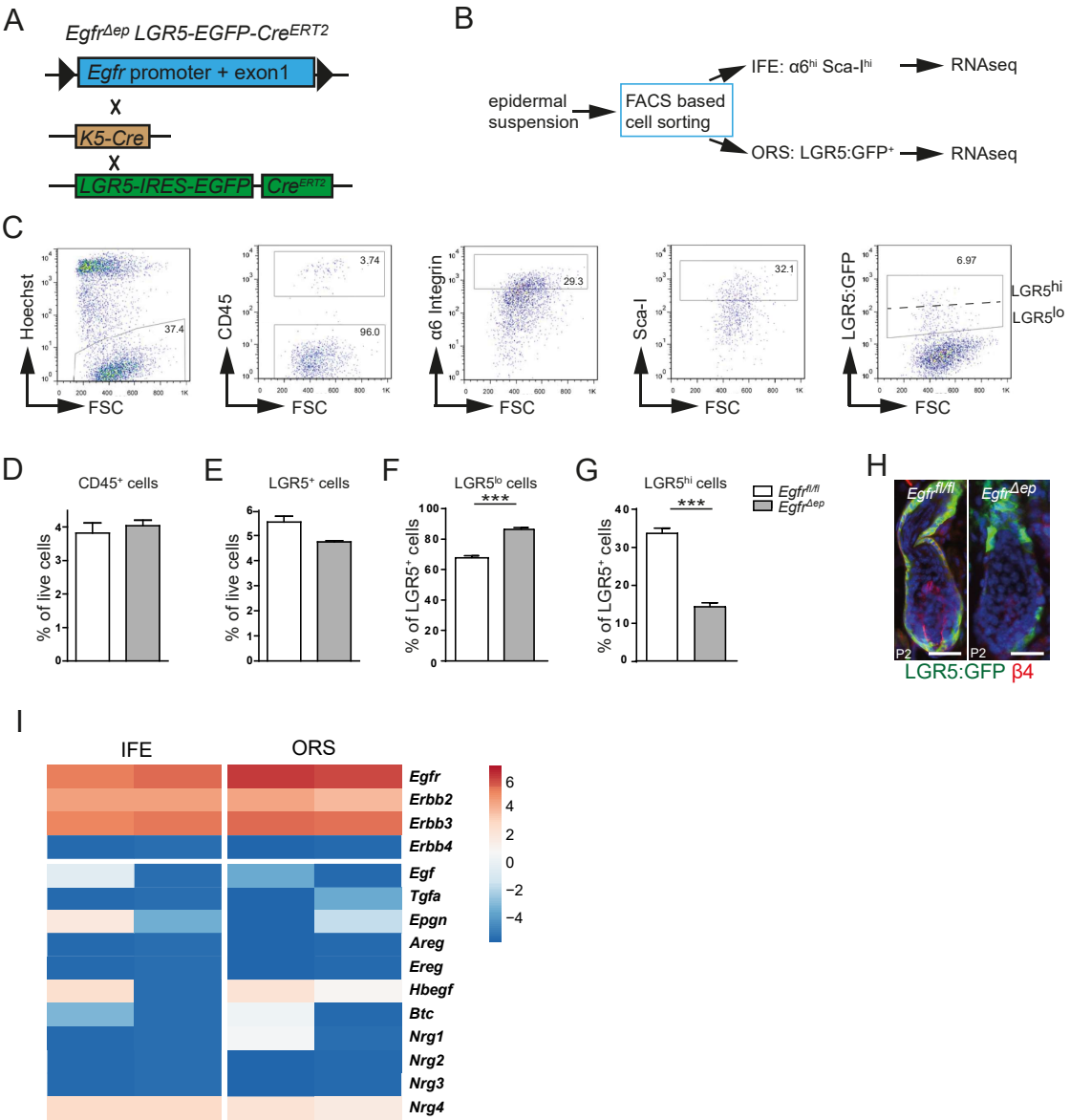
A
Egfr^Δep LGR5-EGFP-CreERT2
Egfr promoter + exon1
X
K5-Cre
X
LGR5-IRES-EGFP
CreERT2
B
epidermal suspension
FACS based cell sorting
IFE: α6hi Sca-Ihi
RNAseq
ORS: LGR5:GFP+
RNAseq
C
Hoechst
FSC
37.4
CD45
3.74
96.0
α6 Integrin
29.3
Sca-I
32.1
LGR5:GFP
6.97
LGR5hi
LGR5lo
D
CD45+ cells
% of live cells
E
LGR5+ cells
% of live cells
F
LGR5lo cells
***
% of LGR5+ cells
G
LGR5hi cells
***
% of LGR5+ cells
Egfrfl/fl
EgfrΔep
H
Egfrfl/fl
EgfrΔep
P2
P2
LGR5:GFP β4
I
IFE
ORS
Egfr
Erbb2
Erbb3
Erbb4
Egf
Tgfa
Epgn
Areg
Ereg
Hbegf
Btc
Nrg1
Nrg2
Nrg3
Nrg4
6
4
2
0
−2
−4

Figure S2. Flow cytometric analysis of newborn mouse skin. Related to Figure 2

(A) Schematic picture of *Egfr*$^{\Delta ep}$ *LGR5-Cre*^{ERT2}*GFP* mice.

(B) Schematic overview of work flow for RNAseq.

(C) FACS gating strategy for cell sorting of IFE and ORS cells from P2 control and *Egfr*$^{\Delta ep}$ *LGR5-Cre*^{ERT2}*GFP* mice.

(D) Quantification of CD45^{+} cells, (E) all LGR5:EGFP^{+} cells, (F) LGR5:EGFP^{lo} cells, and (G) LGR5:EGFP^{hi} cells as from FACS analysis of epidermal cell suspensions of P2 control and *Egfr*$^{\Delta ep}$ *LGR5-Cre*^{ERT2}*GFP* mice. Bars show data from n = 4-5 mice per genotype. Statistical significance was determined by Student's t-test with $p < 0.5$ *, $p < 0.01$ **, $p < 0.005$ ***.

(H) Immunofluorescence staining for GFP (green), ITGB4 (red) and nuclei (blue) from P2 control and *Egfr*$^{\Delta ep}$ *LGR5-Cre*^{ERT2}*GFP* mice, showing HF.

(I) Heat map showing expression of *Erbb* receptors and their ligands in control samples from P2 IFE and P2 ORS. Each column represents one mouse.

Scale bars 20µm unless otherwise stated.

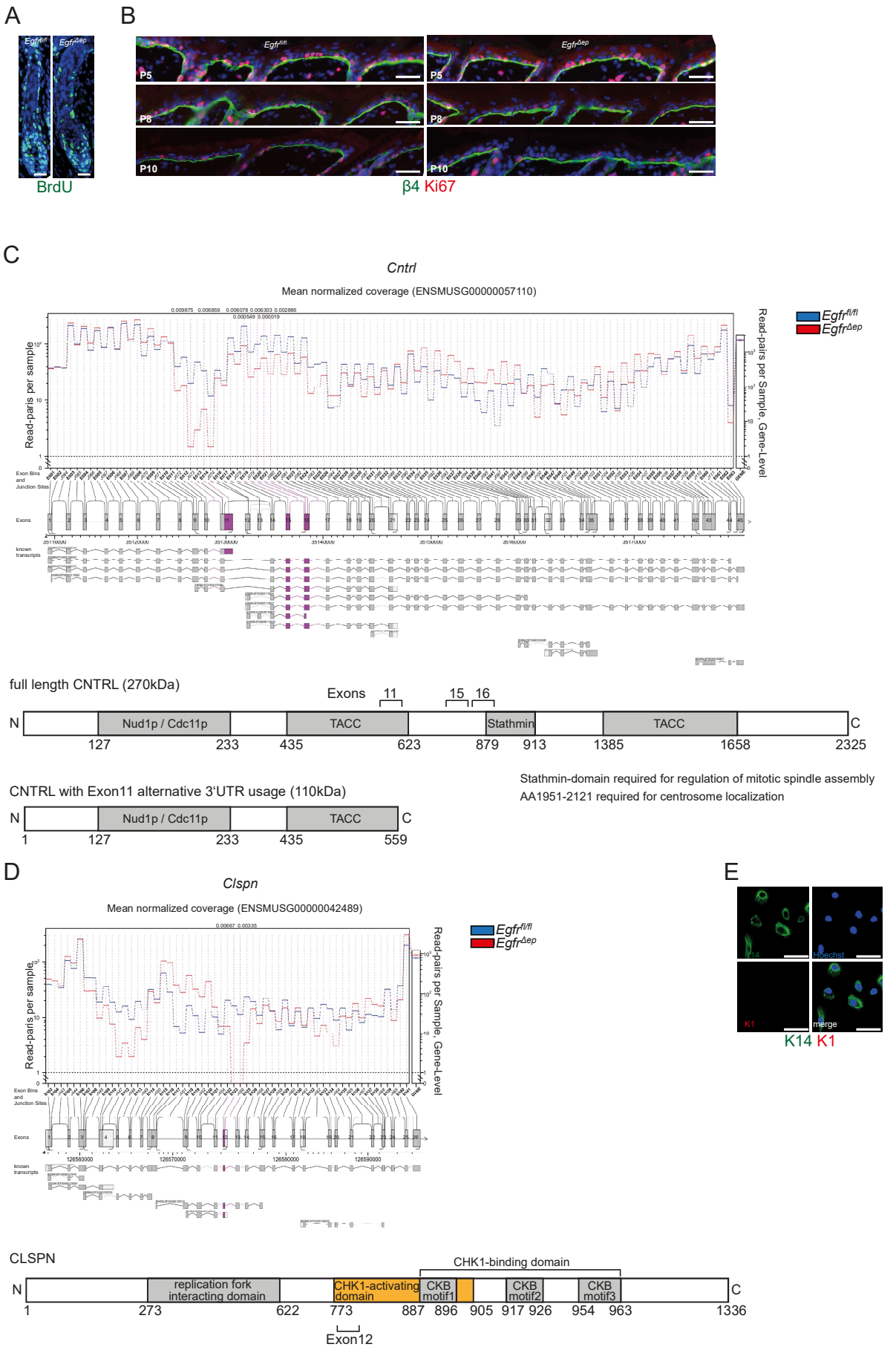
A
B
Egfr^fl/fl
Egfr^Δep
P5
P8
P10
BrdU
β4 Ki67
C
Cntrl
Mean normalized coverage (ENSMUSG00000057110)
Read-pairs per sample
Read-pairs per Sample, Gene-Level
Exon Bins and Junction Sites
Exons
known transcripts
full length CNTRL (270kDa)
Exons 11 15 16
N
Nud1p / Cdc11p
TACC
Stathmin
TACC
C
127 233 435 623 879 913 1385 1658 2325
Stathmin-domain required for regulation of mitotic spindle assembly
AA1951-2121 required for centrosome localization
CNTRL with Exon11 alternative 3'UTR usage (110kDa)
N
Nud1p / Cdc11p
TACC
C
1 127 233 435 559
D
Clspn
Mean normalized coverage (ENSMUSG00000042489)
Read-pairs per sample
Read-pairs per Sample, Gene-Level
Exon Bins and Junction Sites
Exons
known transcripts
126580000 126570000 126580000 126590000
CLSPN
CHK1-binding domain
N
replication fork interacting domain
CHK1-activating domain
CKB motif1
CKB motif2
CKB motif3
C
1 273 622 773 887 896 905 917 926 954 963 1336
Exon12
E
K14
Hoechst
K1
merge
K14 K1

Figure S3. Confirmatory experiments on functional relevance of RNAseq analysis. Related to Figure 3

(A) Immunofluorescence staining for BrdU (green) 24h after pulsing.

(B) Immunofluorescence stainings for ITGB4 Integrin (green), Ki67 (red), and nuclei (blue) from control and *Egfr*$^{\Delta ep}$ mice at indicated timepoints, showing IFE.

(C) JunctionSeq diagram of exon and junction site usage within the *Cntrl* gene (top). Purple coloured exons and junction sites show significantly differentially used elements. Schematic drawing of protein domains of *Cntrl* (bottom).

(D) JunctionSeq diagram of exon and junction site usage within the *Clspn* gene (top). Purple coloured exons and junction sites show significantly differentially used elements. Schematic drawing of protein domains of *Clspn* (bottom).

(E) Immunofluorescence staining for K14 (green), K1 (red) and nuclei (blue) of primary keratinocytes. Bars 10µm.

Scale bars 20µm unless otherwise stated.

Fig. S4, Amberg et al

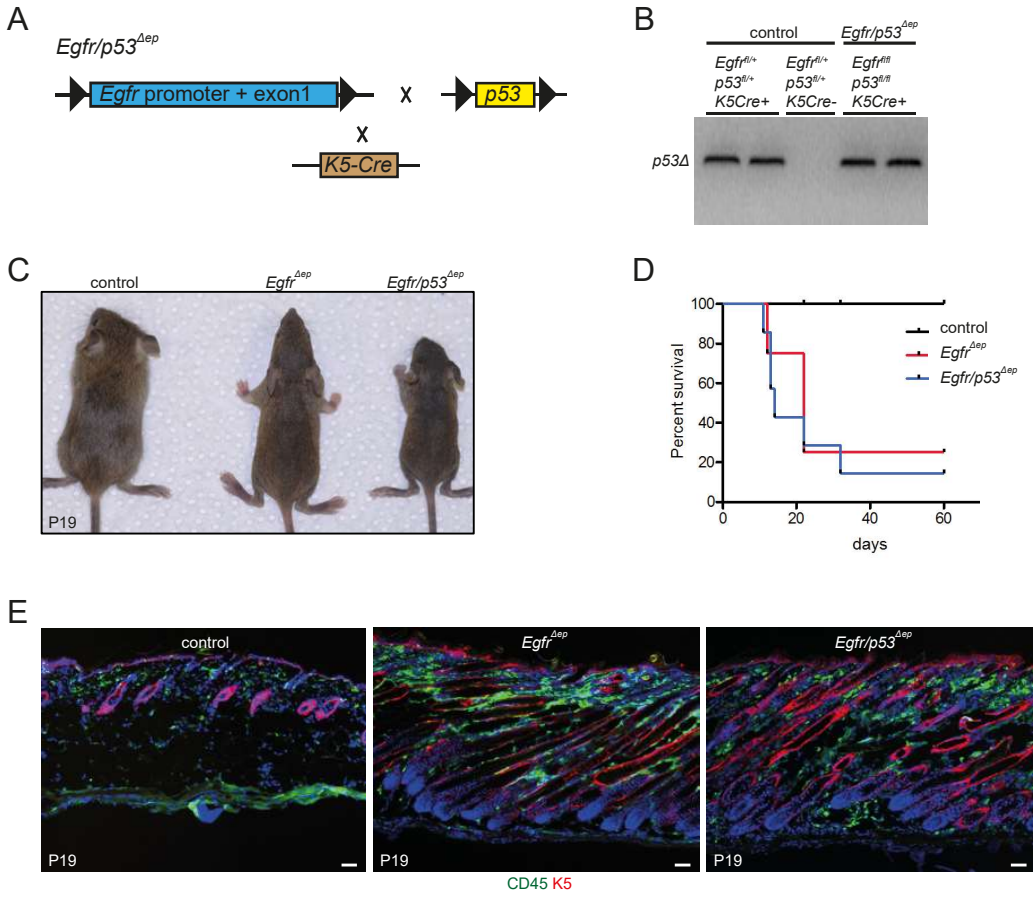

Figure S4. Additional deletion of TP53 does not rescue survival and hair phenotype of mice with EGFR-deficient epidermis. Related to Figure 4

(A) Schematic representation of genetics of *Egfr/p53*$^{\Delta ep}$ mice.
(B) Agarose gel image of *p53* Δallele-specific PCR from control and *Egfr/p53*$^{\Delta ep}$ mice.
(C) Photographs of P19 control, *Egfr*$^{\Delta ep}$ and *Egfr/p53*$^{\Delta ep}$ mice.
(D) Survival curves of control, *Egfr*$^{\Delta ep}$ and *Egfr/p53*$^{\Delta ep}$ mice. Each line shows data from n = 15 mice per genotype.
(E) Immunofluorescence staining of back skin sections for CD45 (green), K5 (red) and nuclei (blue) of P19 control, *Egfr*$^{\Delta ep}$ and *Egfr/p53*$^{\Delta ep}$ mice.

Scale bars 50μm.

Fig. S5, Amberg et al

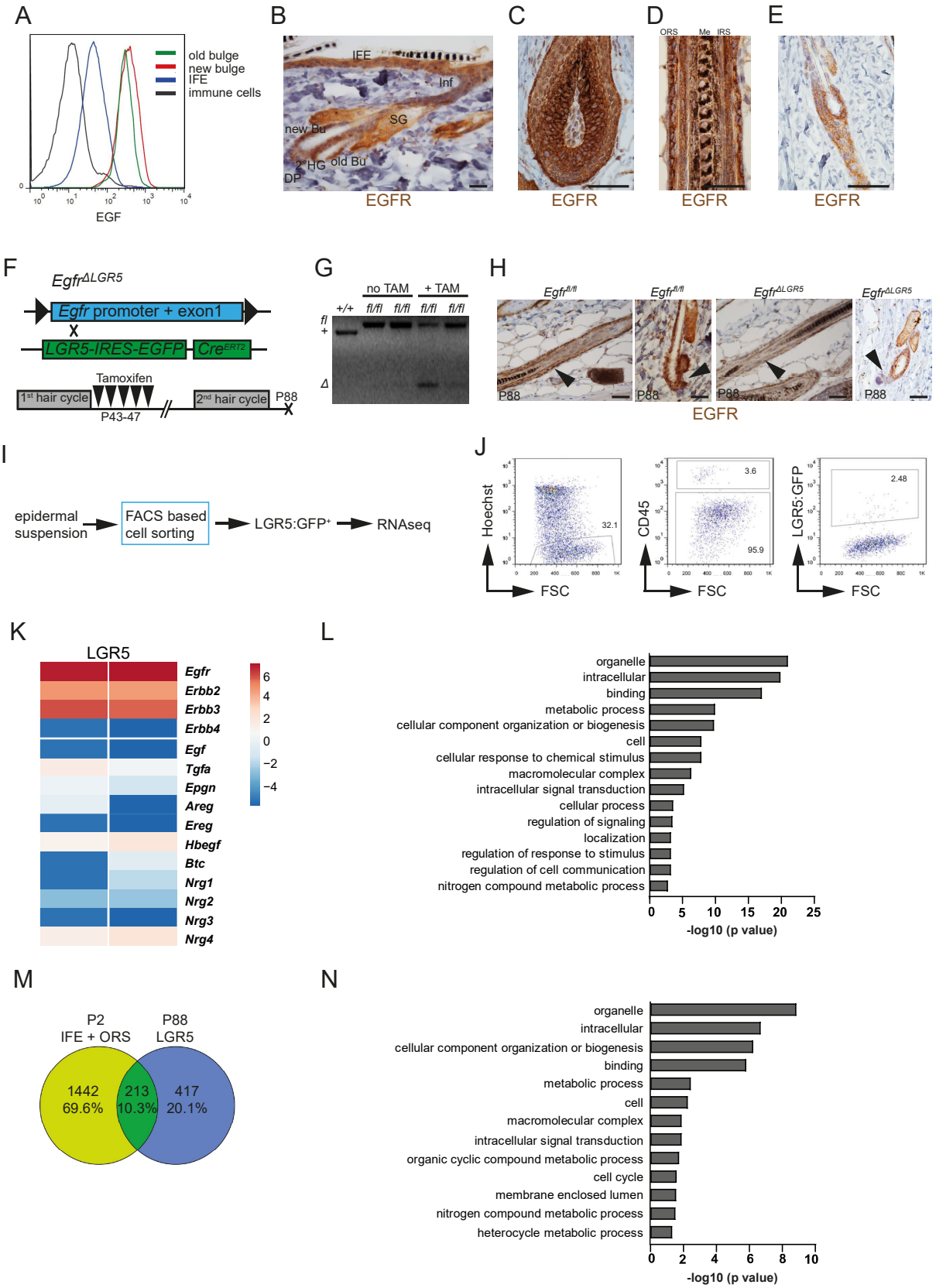

Figure S5. Analysis of localization and function of EGFR in the epidermis of adult mice. Related to Figure 6

(A) Histogram from FACS analysis of P45 mice showing intensity of EGF-A647 for indicated epidermal compartments.

(B) Immunohistochemistry staining of EGFR on a back skin section of an adult control mouse. IFE – interfollicular epidermis; Inf – Infundibulum; SG – sebaceous gland; Bu – bulge; 2°HG – secondary hair germ; DP – dermal papilla.

(C) Immunohistochemistry staining of EGFR on a back skin section of an adult control mouse, showing the matrix of an anagen HF.

(D) Immunohistochemistry staining of EGFR on a back skin section of an adult control mouse, showing the hair shaft of an anagen HF; ORS – outer root sheath; Me – medulla; IRS – inner root sheath.

(E) Immunohistochemistry staining of EGFR on a back skin section of an adult control mouse, showing a catagen HF.

(F) Schematic representation of genetics of *Egfr*$^{\Delta LGR5}$ mice and treatment regimen.

(G) Agarose gel image of *Egfr* Δ-allele specific PCR from back skin of control and *Egfr*$^{\Delta LGR5}$ mice.

(H) Immunohistochemistry staining of back skin sections of P88 control and *Egfr*$^{\Delta LGR5}$ mice, showing anagen and telogen HFs.

(I) Schematic overview of work flow for RNAseq.

(J) FACS gating strategy for cell sorting of LGR5^{+} cells from P88 control and *Egfr*$^{\Delta LGR5}$ mice.

(K) Heat map showing expression of *Erbb* receptors and their ligands from control samples of P88 LGR5^{+} HFSCs. Each column represents one mouse.

(L) Bar diagram of top 15 GO terms of alternatively used exons and junction sites of LGR5^{+} cells from P88 *Egfr*$^{\Delta LGR5}$ mice.

(M) Venn diagram of alternatively spliced genes from P2 IFE + ORS and P88 LGR5^{+} cells.

(N) Bar diagram of GO terms of shared alternatively spliced genes between P2 IFE + ORS and P88 LGR5^{+} cells.

Scale bars 20μm unless otherwise stated.

Transparent Methods

Mice

Mice were kept in the animal facilities of the Medical University of Vienna in accordance with institutional policies and federal guidelines. Animal experiments were approved by the Animal Experimental Ethics Committee of the Medical University of Vienna and the Austrian Federal Ministry of Science and Research (animal license numbers: GZ 66.009/124-BrGT/2003; GZ 66.009/109-BrGT/2003; BMWF-66.009/0073-II/10b/2010; BMWF-66.009/0074-II/10b/2010). $EGFR^{fl/fl}$ mice (Natarajan et al. 2007) were kept in C57BL/6 background for more than 30 generations and were crossed with K5Cre transgenic mice (Tarutani et al. 1997), (LGR5-EGFP-Cre^{ERT2} knock-in mice (Barker et al. 2007) and $p53^{fl/fl}$ mice (Marino et al. 2000). While K5Cre and LGR5-EGFP-Cre^{ERT2} mice were of C57BL/6 background, $p53^{fl/fl}$ mice were of mixed background. Sequences of genotyping primers can be found in Supplemental Table S2.

No phenotypic differences have been identified between male and female mice, thus all experiments were conducted using both genders. Age of analysed mice is indicated in each figure legend.

Embryonic and newborn pups were sacrificed by decapitation. Mice older than P3 were sacrificed by cervical dislocation.

For Tamoxifen-induced deletion of EGFR, 1mg Tamoxifen/mouse (resolved in 10v/v% EtOH (Roth) and 90v/v% sun flower seed oil (Sigma) was injected for 5 consecutive days from P43-47.

Keratinocyte culture

Back skin was surgically removed and subcutaneous adipose tissue was gently removed. Skin was placed dermal-side down on 0.8% Trypsin (diluted in PBS, Sigma) at 37°C for 30min. Epidermis was peeled off under a sterile laminar flow hood, transferred to a 1.5ml Eppendorf tube containing PBS + 2% chelated FCS and chopped into tiny pieces using sterile scissors. This solution was transferred to 15ml Falcon tube and after adding 5ml DNaseI solution (Sigma, #DN25, 250µg/ml in MEM + 8% chelated FCS) incubated on a rotating shaker at 37°C for 45min. 10ml PBS + 2% chelated FCS were added and the solution was pipetted up and down several times and passed over a 70µm cell strainer into a new tube. After centrifugation at 300g for 10min, cells were resuspended in keratinocyte medium (PromoCell, medium constituted according to the manufacturer's instructions), counted and incubated at a concentration of $5x10^4$ cells/well in pre-coated 8-well chamber slides at 32°C (Coating medium: 100ml MEM, 10ml BSA (FractionV 1mg/ml), 1ml 2mM HEPES pH 7.3, 1ml PureCol (Inamed BioMaterials), 1ml 1mg/ml Fibronectin, 1.16ml 100mM $CaCl_2$). 24-36 hours later, medium was changed and cells were allowed to grow for 2-3 more days.

BrdU incorporation assay

For *in vivo* ORS BrdU incorporation assays, newborn mice were injected with 0.625mg BrdU once and sacrificed 24h later. For IFE BrdU incorporation assays, mice of 5, 8, or 10 days of age were injected with BrdU and sacrificed 4h later.

Histology (Sections)

For histological analysis, skin was processed as described previously (Amberg et al. 2015). Briefly, paraffin-embedded skin biopsies were cut into 4µm thin sections and stained with Hematoxylin & Eosin or Fontana Masson according to standard protocols or subjected to immunohistochemistry (IHC) stainings. For IHC, samples were deparaffinized and rehydrated, antigen retrieval was performed using the respective antigen retrieval buffer and an aptum Retriever 2100 antigen retrieval machine. Endogenous peroxidase was blocked by incubation in 3% H_2O_2 in Methanol for 10min, followed by biotin blocking using Endogenous Biotin Blocking Kit (LifeTech) for 20min each and blocking of unspecific antibody binding using PBS supplemented with 1% BSA, 5% Horse Serum and 0.1% Triton X-100 for 1h at room temperature before adding primary antibodies. In case primary antibodies were raised in mouse, blocking was performed using M.O.M. kit (mouse on mouse, Vector Laboratories, FKM-2201). Primary antibodies were incubated in antibody blocking buffer (1% BSA, 5% Horse Serum, 0.1% TritonX-100 in PBS) over night at 4°C. Biotinylated secondary antibodies were diluted 1:500 in antibody blocking buffer and incubated at room temperature for 1h, followed by Streptavidin incubation for 30min. After DAB reaction was performed, sections were counterstained with Gill's Hematoxylin, dehydrated and embedded using Entellan.

For BrdU stainings, 4µm paraffin sections were incubated with 1N HCl at 37°C for 1h, blocked with antibody blocking buffer and stained with anti-BrdU antibody (BD, 1:50) at 4°C over night. Secondary antibody was diluted 1:500 in blocking buffer, and together with Hoechst (1µg/ml) incubated for 1h at room temperature, before mounting with DAKO mounting medium.

In order to obtain frozen samples, skin biopsies were embedded in Sakura O.C.T., frozen on dry ice and stored at -80°C until sectioning in a Histocom cryomicrotome. 6µm sections were stored at -80°C until further use. For GFP staining, fresh skin biopsies were fixed in 4% PFA for 2h and incubated in 30% sucrose in PBS at 4°C over night prior to embedding and freezing in Sakura O.C.T. Frozen sections were thawed, blocked with 4% PFA for 10min at room temperature, incubated with antibody blocking buffer for 1h at room temperature and stained with primary antibody diluted in antibody blocking buffer at 4°C over night. Secondary antibodies were diluted 1:500 in blocking buffer, and together with Hoechst (1µg/ml) incubated for 1h at room temperature, before mounting with DAKO mounting medium.

Sections were all imaged at a Nikon Eclipse i80 microscope using NIS Elements software (equipped with a Nikon DS-U2 camera for brightfield microscopy and a Nikon DS-Qi2 camera for epifluorescence microscopy), a Zeiss Axio Imager using Axio Vision software or a Zeiss LSM700 confocal microscope using ZEN2010. Images were further processed using Photoshop5.

Histology (Transmission electron microscopy)
Back skin biopsies were cut into pieces of 1x1 mm, fixed in 3% glutaraldehyde (AGAR Scientific) in 0.1M caco buffer (AGAR Scientific), post-fixed in 1 % osmium tetroxide (EMS), dehydrated and embedded in Agar Low Viscosity resin (AGAR Scientific). 80nm ultrathin sections were performed at a Reichert-Jung Ultracut E microtome and stored on copper grids (AGAR Scientific).Sections were further stained in 0.5% uranyl acetate (Laurylab) and 3% lead citrate (Laurylab) before imaging at a TEM Philips *I* FEI EM 208 or a TEM ZEISS EM 902.
Histology (primary keratinocytes)
Medium was removed and cells were washed with PBS 3 times. Cells were incubated with 4% PFA for 30min at RT, washed with PBS 3 times and staining procedure was identical to histological sections. Phalloidin-A488 was diluted 1:1000. Images were acquired at a Zeiss LSM700 confocal microscope, using ZEN2010 software.

Flow cytometry
Epidermal cell suspensions were generated by surgically removing the trunk skin and gently scraping off subcutaneous adipose tissue. Skin was then placed on DMEM (Gibco) containing 2mM EDTA and 0.25% Trypsin (Gibco) at 4°C over night. Next day, epidermis was softly scraped off and further dissociated into single cells by pipetting up and down after adding DMEM containing 2% chelexed FCS (Sigma). Cells were filtered using 70µm and 40µm cell strainers (BD), centrifuged at 300g for 10min, and washed with PBS (Sigma) containing 2% chelexed FCS twice before staining. Epidermal single cell suspensions were incubated with the following antibodies: a6-PE (BD, 1:50), Scal-PECy7 (Biolegend, 1:100), CD45-APCCy7 (BD, 1:200), CD34-biotinylated (eBioscience, 1:50), Streptavidin-APC or Streptavidin-A700 (BD or LifeTech, 1:400). A647-labelled EGF was purchased from LifeTechnologies and incubated in a dilution of 1:20 for 30min on ice in an additional step after antibody staining. Dead cell exclusion was performed using Hoechst (1µg/ml). BrdU analysis was performed according to the manufacturer's instructions (BD APC BrdU Flow Kit, Cat# 552598). For evaluation of $BrdU^+$ cell numbers and intensity measurement of EGF-A647, a BD Fortessa cytometer with BD FACSDiva software was used. Further analysis was conducted using FlowJo (Trestar) software. Cell sorting of IFE and ORS cell populations from P2 skin, as well as of P88 $LGR5^+$ HFSCs was performed using a BD AriaI and BD FACSDiva software.

RNA isolation
Approx. 8,000 IFE and 1,000 $LGR5^+$ keratinocytes were sorted into RNA Extraction Buffer of the PicoPure RNA Isolation Kit (Arcturus), incubated at 42°C for 30min and centrifuged at 800g for 2 min. Supernatants were transferred into new tubes and stored at -80°C until further RNA purification according to the manufacturer's instructions, despite the last step. For RNA elution, we did not use the provided Elution Buffer, but RNase-free water in order to be able to measure RNA quality with the BioAnalyzer (Total Eukaryote RNA Pico Kit, Agilent, according to the manufacturer's instructions).

Library Preparation
RNA samples with RIN > 8.0 were used for RNAsequencing. Libraries were prepared using SMARTer Ultra Kit (Clontech, #63482) and Low Input Library Prep Kit (Clontech, #634947) according to the manufacturer's instructions.

Libraries were subjected to paired-end 150bp read RNAseq at the Biomedical Sequencing facility of the CEMM (Vienna, Austria) using the HiSeq2500 (Illumina Inc.).

RNAseq analysis
TopHat2 algorithm was used to align raw RNA-seq data to mm10 (Kim et al. 2013). Differentially expressed genes were identified using DeSeq2 algorithm (Love et al. 2014). An adjusted P<0.1 was defined as cutoff for differentially expressed genes. Gene Ontology analyses were performed using Ontologizer software (Bauer et al. 2008). Differential splicing was analyzed using the R package JunctionSeq (Hartley and Mullikin 2016).

Data availability
Raw data from RNAseq experiments are available at the NCBI Gene Expression Omnibus (GEO) with the GEO accession number GSE128436.

qRT-PCR
cDNA was generated using VILO cDNA synthesis kit (Life Technologies) according to the manufacturer's protocol. cDNA was stored at -20°C until further use. qRT-PCR was run with SYBR green (Peqlab) on an ABI7500 qRT-PCR machine under the following conditions: an initial incubation at 50°C for 20sec and 95°C for 10 min followed by 40 cycles of 95°C for 15sec, 54°C for 1 min. Relative quantification of RNA was calculated by the $\Delta\Delta C_t$ method using *Gapdh* as reference gene. Primer sequences were purchased from MWG Eurofins.

Statistics
Data were analysed by two-tailed Student's t test, Kruskal-Wallis test or multiple t-tests according to Two-stage linear step-up procedure of Benjamini, Krieger and Yekutieli with Q = 1%. Error bars represent ±SD. Exact number of animals and samples are stated in the figure legends. P values less than 0.05 were considered significant, with $p< 0.05$ *, $p < 0.01$ **, $p < 0.001$ ***.

Polar Plots
Polar plots were generated using R software.

Supplemental References

Amberg N, Holcmann M, Glitzner E, Novoszel P, Stulnig G, Sibilia M. 2015. Mouse Models of Nonmelanoma Skin Cancer. in *Methods in Molecular Biology*, pp. 217-250. Springer Science + Business Media.

Barker N, van Es JH, Kuipers J, Kujala P, van den Born M, Cozijnsen M, Haegebarth A, Korving J, Begthel H, Peters PJ et al. 2007. Identification of stem cells in small intestine and colon by marker gene Lgr5. *Nature* **449**: 1003-1007.

Bauer S, Grossmann S, Vingron M, Robinson PN. 2008. Ontologizer 2.0--a multifunctional tool for GO term enrichment analysis and data exploration. *Bioinformatics* **24**: 1650-1651.

Hartley SW, Mullikin JC. 2016. Detection and visualization of differential splicing in RNA-Seq data with JunctionSeq. *Nucleic Acids Res* **44**: e127.

Kim D, Pertea G, Trapnell C, Pimentel H, Kelley R, Salzberg SL. 2013. TopHat2: accurate alignment of transcriptomes in the presence of insertions, deletions and gene fusions. *Genome Biol* **14**: R36.

Love MI, Huber W, Anders S. 2014. Moderated estimation of fold change and dispersion for RNA-seq data with DESeq2. *Genome Biol* **15**: 550.

Marino S, Vooijs M, van Der Gulden H, Jonkers J, Berns A. 2000. Induction of medulloblastomas in p53-null mutant mice by somatic inactivation of Rb in the external granular layer cells of the cerebellum. *Genes Dev* **14**: 994-1004.

Natarajan A, Wagner B, Sibilia M. 2007. The EGF receptor is required for efficient liver regeneration. *Proceedings of the National Academy of Sciences* **104**: 17081-17086.

Tarutani M, Itami S, Okabe M, Ikawa M, Tezuka T, Yoshikawa K, Kinoshita T, Takeda J. 1997. Tissue-specific knockout of the mouse Pig-a gene reveals important roles for GPI-anchored proteins in skin development. *Proceedings of the National Academy of Sciences* **94**: 7400-7405.